

# Electrochemical studies on the reduction behaviour of ruthenium nitrosyl ions in nitric acid medium

Pravati Swain · C. Mallika · Ch. Jagadeeswara Rao ·  
U. Kamachi Mudali · R. Natarajan

Received: 16 June 2014 / Accepted: 22 September 2014 / Published online: 7 October 2014  
© Springer Science+Business Media Dordrecht 2014

**Abstract** To understand the low recovery of ruthenium from ruthenium nitrosyl nitrate solution by electro-deposition technique, electro-reduction behaviour of ruthenium nitrosyl complex  $[\text{Ru}^{\text{II}}\text{-NO}^+]^{3+}$  in nitric acid medium was investigated using the potentiostatic electrolysis techniques, cyclic voltammetry and chronopotentiometry at Pt and glassy carbon working electrodes. Reduction of  $[\text{RuNO}]^{3+}$  was found to be quasi-reversible, one electron transfer process at both the electrodes. The diffusion coefficient ( $D_0$ ) of  $[\text{RuNO}]^{3+}$  species estimated by these techniques was in the order of  $10^{-8} \text{ cm}^2 \text{ s}^{-1}$  and the heterogeneous electron transfer rate constant ( $k_s$ ) for the reduction of  $[\text{RuNO}]^{3+}$  was estimated to be about  $10^{-5} \text{ cm s}^{-1}$  using Klingler and Kochi equation. The very low diffusion coefficient value and the low separation percentage of Ru from ruthenium nitrosyl nitrate solution by electro-deposition technique are attributed to the existence of Ru(II) in different stable complexes instead of bare Ru(II) ions, in nitric acid medium.

**Keywords** Ruthenium nitrosyl complexes · Glassy carbon electrode · Electroanalytical technique · Electro-reduction · Kinetic parameters

## 1 Introduction

The platinum group element, ruthenium is produced in relatively large quantity during the fission of plutonium-rich nuclear fuels in fast breeder reactors. Ruthenium creates problems during the aqueous reprocessing of spent fuels by PUREX process as well as in the management of high level liquid waste (HLLW), owing to the formation of large number of complexes in nitric acid medium and also highly volatile radiotoxic  $\text{RuO}_4$ . The complexity in the chemistry of Ru is because of the large range of its oxidation states from 0 to +8 and also -2. Considerable effort has been made to investigate the chemistry of ruthenium in nitric acid medium [1–6]. Ruthenium complexes formed in nitric acid can be represented by the general formula  $[\text{RuNO}(\text{NO}_3)_x(\text{NO}_2)_y(\text{OH})_z(\text{H}_2\text{O})_{5-x-y-z}]^{3-x-y-z}$ . Ruthenium can also form nitrosyl (RuNO) complexes in nitric acid, which have the ability to exchange ligands. The composition of the solution containing a mixture of ruthenium nitrosyl complexes depends on the concentration of acid, temperature, ruthenium species present initially and the time elapsed since its formation because of the inter-conversion of different nitrosyl complexes with different half times [7]. In the PUREX process, for the separation of U and Pu from the fission products by solvent extraction, some of the complexes of Ru (mainly trinitrato ruthenium nitrosyl complexes) are extracted into the organic phase, 30 % tributyl phosphate (TBP) along with U and Pu. Reduction of  $[\text{Ru}(\text{NO})]^{3+}$  complexes to the lower oxidation state namely  $[\text{Ru}(\text{NO})]^{2+}$  would facilitate the separation of Ru from U and Pu during PUREX process. Among the methods reported in the literature [8] for the separation of Ru from radioactive liquid waste, electrochemical method is advantageous, because this method is simple and requires neither the addition of external

P. Swain · C. Mallika (✉) · U. Kamachi Mudali · R. Natarajan  
Reprocessing Group, Indira Gandhi Centre for Atomic Research,  
Kalpakkam 603 102, India  
e-mail: mallika@igcar.gov.in

Ch. Jagadeeswara Rao  
Corrosion Science and Technology Group, Indira Gandhi Centre  
for Atomic Research, Kalpakkam 603 102, India

reagents nor complicates the reprocessing steps and waste management operation. In the electrochemical method, Ru can be separated either by deposition as metal on the cathode [9–14] or by oxidation to  $\text{RuO}_4$  at the anode [15–20]. Separation of Ru was quantitative in the electro-oxidation method [20]; however, separation percentage of Ru by electro-deposition technique was found to be very low and a large portion remained in the solution. In order to understand the low recovery of Ru by electro-deposition technique, it is desirable to study the behaviour of the lower oxidation states of Ru. The electrolytic reduction of ruthenium nitrosyl complexes had been investigated by several researchers in various electrolytes [21–26]. Nevertheless, there is no reliable report on the reduction of ruthenium nitrosyl complexes in nitric acid medium, except a single study on the oxidation of ruthenium nitrosyl complexes in nitric acid media [27]. In the present study, the reduction behaviour of ruthenium nitrosyl complex  $[\text{Ru}^{\text{II}}\text{-NO}^+]^{3+}$  and its kinetics in nitric acid medium have been investigated using the potentiostatic electrolysis techniques, cyclic voltammetry (CV) and chronopotentiometry (CP), at Pt and glassy carbon (GC) working electrodes.

## 2 Experimental

For performing electrochemical measurements, a standard solution of ruthenium nitrosyl  $[\text{RuNO}]^{3+}$  containing 40 mM of Ru in 1 M nitric acid was prepared by diluting the commercially available ruthenium nitrosyl nitrate solution (1.7 % Ru in 9 M nitric acid, supplied by M/s. Arora Matthey Ltd, Kolkata). Nitric acid (AR grade, 69–71 %) used in all the experiments was supplied by M/s. Fischer Chemicals Ltd, Chennai. Electrochemical measurements on the reduction of ruthenium nitrosyl complex were conducted using the cell configuration shown in Fig. 1. A 1-mm diameter platinum wire (surface area (SA):  $0.42 \text{ cm}^2$ ) and a 3-mm diameter GC rod (SA:  $0.44 \text{ cm}^2$ ; supplied by M/s. Metrohm India) were used independently

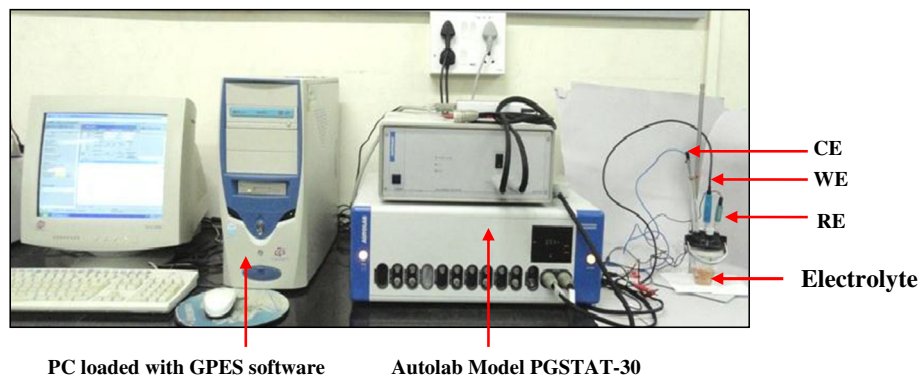
as the working electrodes. A Pt foil (SA:  $1.2 \text{ cm}^2$ ) and Ag/AgCl were used as the counter and reference electrodes, respectively. The GC working electrode was finely polished using alumina slurry on a microcloth pad. It was cleaned before and after polishing by ultrasonication in distilled water for about 300 s in order to remove the adhered particles. Further degreasing and rinsing were carried out in acetone and distilled water, respectively and was gently dried with a hot air blower. Ruthenium nitrosyl nitrate solution (25 ml) containing 5, 20 or 40 mM ruthenium in 1 M nitric acid served as the electrolyte. The voltammograms were recorded at different scan rates in the range  $10\text{--}100 \text{ mV s}^{-1}$ . De-oxygenation of the test solutions prior to the scans was done by flushing the cell assembly with argon gas and the results were analysed after IR compensation. Likewise, chronopotentiograms were recorded by applying very small increments of current to the cell. Reduction of ruthenium nitrosyl complex,  $[\text{RuNO}]^{3+}$  was carried out by chronoamperometry and the reduced Ru species was characterized by UV–Visible spectrophotometry. Chemito Spectrascan, UV 2600 double beam UV–Vis spectrophotometer was used for recording the spectra. Bulk electrolysis was conducted in a divided electrolytic cell using glass frit as the diaphragm. Pt mesh of surface area, 34 and  $\sim 20 \text{ cm}^2$  were used as the working and counter electrodes, respectively, along with the reference electrode. The potentiostatic and constant potential electro-oxidation studies were carried out using Comprehensive Autolab (Model PGSTAT-30; M/s. Eco-Chemie, the Netherlands) electrochemical system equipped with General Purpose Electrochemical Software.

## 3 Results and discussion

### 3.1 Reduction potential and cyclic voltammograms of $[\text{RuNO}]^{3+}$ complex in nitric acid medium

The cyclic voltammograms of 40 mM of Ru in  $[\text{RuNO}]^{3+}$  solution in 1 M nitric acid, recorded at the scan rate of

**Fig. 1** Cell assembly and electrochemical work station used for electrochemical studies



50  $\text{mV s}^{-1}$  using platinum working electrode, at 298 K are shown in Fig. 2. The voltammograms were recorded, starting with the cathodic scan over the potential range 1.0 to  $-0.3$  V against Ag/AgCl reference electrode. A distinct reduction peak ( $I_c$ ) observed at about 0.4 V and the oxidation peak ( $I_a$ ) at about 0.6 V (vs. Ag/AgCl) corresponded to the redox couple  $[\text{RuNO}]^{3+}/[\text{RuNO}]^{2+}$ . In addition to this peak, there was a surge in the cathodic current at 0.04 V, culminating into a small hump at about  $-0.16$  V during the cathodic scan, which could be attributed to the reduction of  $[\text{RuNO}]^{2+}$  to Ru metal. The second oxidation peak observed at 0.95 V, when the CV was recorded at Pt working electrode over the potential region 1.2–0.0 V (vs. Ag/AgCl) is shown in Fig. 3. This oxidation peak could be ascribed to the oxidation of  $[\text{RuNO}]^{3+}$  to  $[\text{RuNO}]^{4+}$ . Cyclic voltammograms of 5 and 20 mM of  $[\text{RuNO}]^{3+}$  solutions in 1 M  $\text{HNO}_3$  were also recorded, with the scan rate of 50  $\text{mV s}^{-1}$ . The reduction peak current was observed to increase with increasing concentration of ruthenium (Fig. 3).

Ruthenium nitrosyl complexes with the general formula  $[\text{RuNO}(\text{NO}_3)_x(\text{NO}_2)_y(\text{OH})_z(\text{H}_2\text{O})_{5-x-y-z}]^{3-x-y-z}$  may be cationic, anionic or neutral complexes depending on the values of  $x$ ,  $y$  and  $z$ . The NO ligand in the  $[\text{RuNO}]^{3+}$  complex is considered to bond formally as  $\text{NO}^+$  by donating an electron to Ru(III). The diamagnetism exhibited by  $[\text{RuNO}]^{3+}$  complexes ascertain this; hence, the complex is equivalent to a bivalent Ru(II) containing  $\text{NO}^+$  and the most probable description for the moiety would be  $[\text{Ru}^{\text{II}}\text{NO}^+]^{3+}$  [28, 29]. The bonding electrons are partially donated from the filled metal d-orbitals to the empty ligand NO  $\pi^*$  orbital (this process is known as metal-to-ligand  $\pi$ -bonding or back-bonding). Six coordinated ruthenium

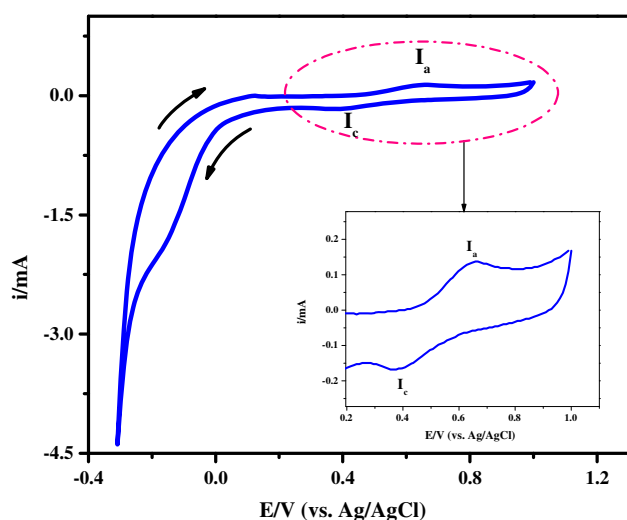


**Fig. 2** Cyclic voltammogram of 40 mM ruthenium nitrosyl ( $[\text{RuNO}]^{3+}$ ) solution in 1 M  $\text{HNO}_3$ ; scan rate: 50  $\text{mV s}^{-1}$ ; working electrode: Pt; temperature: 298 K

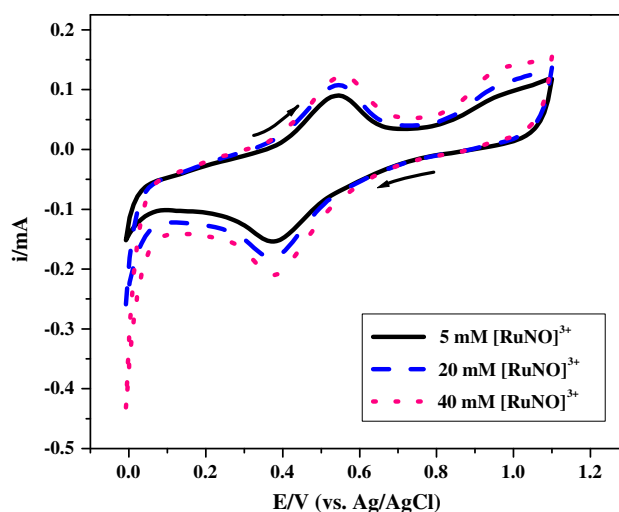


**Fig. 3** Cyclic voltammograms of  $[\text{RuNO}]^{3+}$  solution ([Ru]: 5, 20 and 40 mM) in 1 M  $\text{HNO}_3$ , recorded using 50  $\text{mV s}^{-1}$  scan rate at Pt working electrode and at 298 K

complexes are extremely stable because  $\text{Ru}^{2+}$  with the  $d^6$  configuration obeys the 18-electron rule, when octahedrally coordinated and additionally stabilized by  $\pi$ -bonding ligands. Based on molecular orbital (MO) analysis using the density functional theory (DFT) and from the reduction product analysis, it has been reported that during the electrochemical reduction of ruthenium nitrosyl complexes, the first site of reduction would be assigned to the  $\text{NO}^+$  to NO at the coordinated  $\text{NO}^+$  (Eq. 1) [30]. Further reduction might occur at the ruthenium centre and the possible reduction is  $\text{Ru}^{2+}$  to Ru metal (i.e.  $\text{Ru}^{2+} + 2e^- = \text{Ru}^0$ ). It is also reported that the reduction potential for  $\text{NO}^+/\text{NO}$  in Ru nitrosyl complexes is sensitive to the nature of trans ligand. As the  $\pi$  acidity of ligand increases, more nitrosonium character is imposed in the NO ligand and, thus, its reduction becomes easier [21–24, 30]. In the present work, the reduction wave ( $I_c$ ) and the corresponding oxidation wave ( $I_a$ ) were assigned to the reduction of  $[\text{Ru}^{\text{II}}\text{NO}^+]^{3+}$  to  $[\text{Ru}^{\text{II}}\text{NO}]^{2+}$ .



Gomes et al. [24] reported that the  $\text{NO}^+/\text{NO}$  reduction process in some ruthenium nitrosyl complexes is reversible within the time scale of experiments, suggesting the reasonable stability of some of the reduced complexes; however, Doro et al. [31] observed that this reduction process for some complexes is irreversible and it depends on the experimental conditions such as scan rate and temperature.

The peak corresponding to the reduction of ruthenium nitrosyl complex was validated by carrying out a controlled potential electrolysis of a solution containing 160 ppm of Ru in 1 M nitric acid at 0.4 V. The UV–Visible spectra of the electrolyte solutions recorded before and after

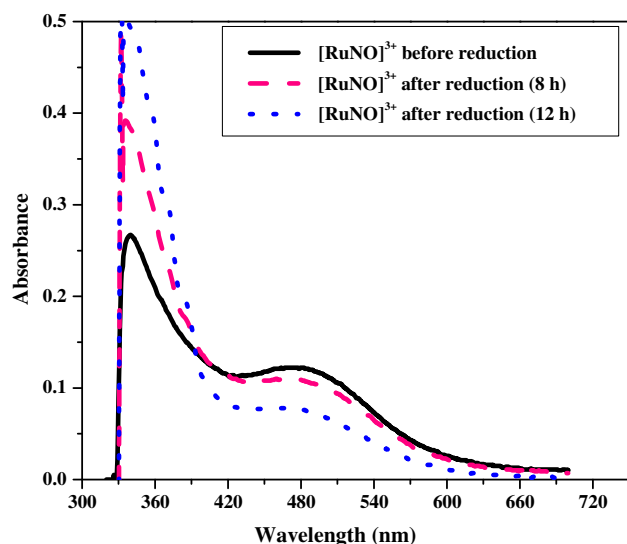


**Fig. 4** UV–Visible spectra of  $[\text{RuNO}]^{3+}$  solution in 1 M  $\text{HNO}_3$  before and after electrolysis

electrolysis are reproduced in Fig. 4. Tfouni et al. [30] observed the spectra of ruthenium nitrosyl complexes to display a broad absorption band in the range 400–500 nm and they have attributed it to metal-to-ligand charge transfer (MLCT),  $\text{Ru}^{\text{II}} \rightarrow \text{NO}$  transition; another higher absorption peak with high intensity in the range 300–350 nm, recorded by them was ascribed to d–d transition. In the present study also, similar observations were recorded. With increase in the duration of electrolysis, intensity of the characteristic absorption band owing to MLCT transition at 473 nm was found to decrease, which might be due to the destabilization of metal centre caused by the decrease in back-bonding because of  $\text{NO}^+$  reduction [32]. Increase in the intensity of the absorption band at about 340 nm and generation of new shoulders at 387, 370 and 358 nm were also observed as electrolysis proceeded.

### 3.2 Estimation of kinetic parameters for the reduction of ruthenium nitrosyl complexes

If the rate of an electrochemical process is controlled by diffusion (mass transfer) and not by charge transfer kinetics, then the process is called as reversible process. In a reversible process, the charge transfer is rapid and the slow mass transfer is the rate determining step. The key criterion for a reversible charge transfer process is that the peak potential,  $E_p$  is independent of scan rate ( $v$ ) and

$$E_{p,c} - E_{p,a} = 1.857 RT/\alpha nF, \quad (2)$$

where  $E_{p,c}$  and  $E_{p,a}$  are the cathodic and anodic peak potentials, respectively,  $R$  is the gas constant,  $T$  is the absolute temperature (K),  $\alpha$  is charge transfer coefficient,

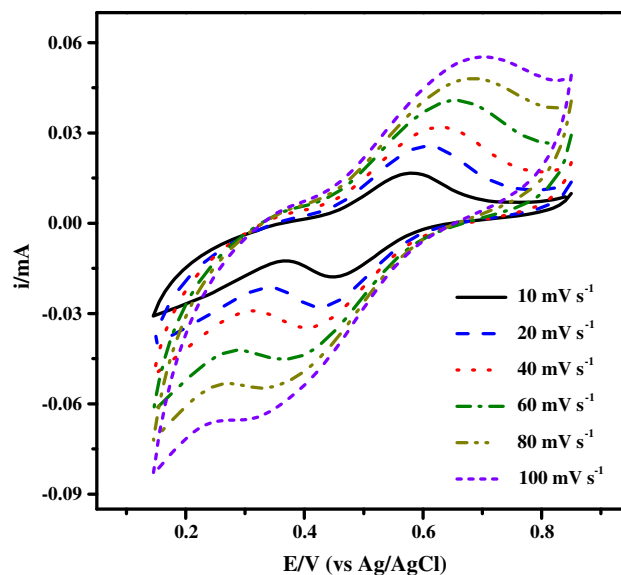


**Fig. 5** Cyclic voltammograms of 40 mM of ruthenium nitrosyl solution in 1 M  $\text{HNO}_3$  recorded at Pt electrode with different scan rates (i.e. 10–100  $\text{mV s}^{-1}$ ); T: 298 K

$n$  is the number of electrons involved in the charge transfer reaction and  $F$  is the Faraday constant.

The reversibility of the electrode processes corresponding to the peaks  $I_c$  and  $I_a$  in Fig. 2 was examined by evaluating the effect of scan rates on the current–potential behaviour, in the electro-reduction of ruthenium nitrosyl ions. Figure 5 represents all the scans from 10 to 100  $\text{mV s}^{-1}$  for the reduction of 40 mM of  $[\text{RuNO}]^{3+}$  solution in 1 M nitric acid, within the selective potential window of 0.15–0.85 V at 298 K. This figure reveals that the cathodic peak potential,  $E_{p,c}$  shifted significantly from 0.46 to 0.39 V (vs. Ag/AgCl) as the scan rate was increased from 10 to 100  $\text{mV s}^{-1}$ , which is not the characteristic of a reversible reaction. The peak parameters measured from the cyclic voltammograms in Fig. 5 are tabulated in Table 1.

If the electrochemical process is controlled mainly by charge transfer kinetics, then the process is called as irreversible process. The important criterion for the irreversible charge transfer kinetics is the shift in the peak potential with scan rate. A relation between the cathodic diffusion peak current,  $i_{p,c}$  and the scan rate, given by Bard and Faulkner [33] is

$$i_{p,c} = 0.496 nFAC_0 \sqrt{\frac{D_0(\alpha n_\alpha)Fv}{RT}}, \quad (3)$$

where  $A$  is area of the electrode (in  $\text{cm}^2$ ),  $C_0$  is the bulk concentration of electro-active species ( $\text{mol cm}^{-3}$ ),  $v$  is the scan rate ( $\text{mV s}^{-1}$ ),  $D_0$  is the diffusion coefficient ( $\text{cm}^2 \text{s}^{-1}$ ) and  $n_\alpha$  is number of electrons transferred in rate determining step.

**Table 1** Peak parameters obtained from the CVs for 40 mM [RuNO]<sup>3+</sup> solution in 1 M HNO<sub>3</sub> recorded with Pt working electrode

Scan rate/mV s <sup>-1</sup>	E <sub>p,c</sub> /V	i <sub>p,c</sub> /A	E <sub>p,a</sub> /V	(E <sub>p,a</sub> - E <sub>p,c</sub> )/V	[1/2(E <sub>p,c</sub> + E <sub>p,a</sub> )]/V
10	0.457	-9.4 × 10 <sup>-6</sup>	0.578	0.121	0.52
20	0.436	-1.2 × 10 <sup>-5</sup>	0.599	0.163	0.52
40	0.428	-1.4 × 10 <sup>-5</sup>	0.618	0.190	0.52
60	0.407	-1.5 × 10 <sup>-5</sup>	0.637	0.230	0.52
80	0.395	-1.6 × 10 <sup>-5</sup>	0.659	0.264	0.53
100	0.387	-1.7 × 10 <sup>-5</sup>	0.675	0.288	0.53

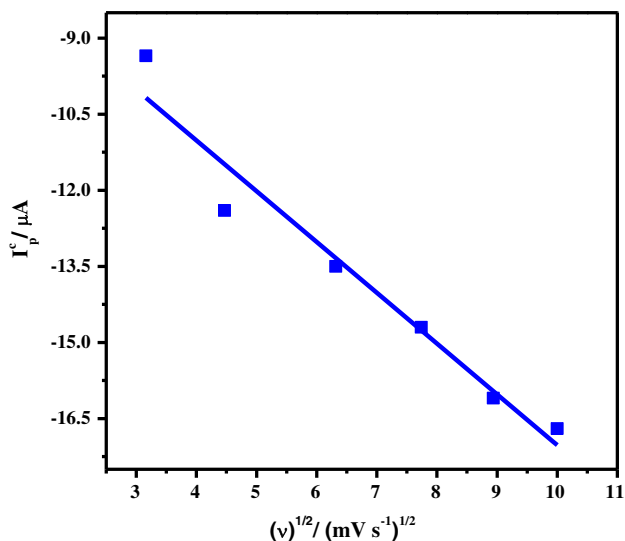


**Fig. 6** Plot of peak current against square root of scan rate for the reduction of 40 mM of Ru in [RuNO]<sup>3+</sup> solution; [HNO<sub>3</sub>]: 1 M

The value of diffusion coefficient of [RuNO]<sup>3+</sup> ion calculated using Eq. (3) and from the slope of the plot of *i*<sub>p,c</sub> against square root of scan rate (Fig. 6) was 2.95 × 10<sup>-8</sup> cm<sup>2</sup> s<sup>-1</sup>. This very low diffusion coefficient value indicates the complexing nature of Ru(II). The existence of Ru(II) in different complexes instead of bare Ru(II) ions, limits the recovery of ruthenium from aqueous solutions. Further, Ru(II) undergoes two step reduction to Ru and the second reduction occurs in the decomposition range of the aqueous solution, which controls the separation of Ru by electro-deposition.

For the reduction of [RuNO]<sup>3+</sup> ions in 1 M nitric acid medium, peak potential shift and broadening of peak shape with scan rate were observed in cyclic voltammetric runs. The difference between the cathodic and anodic peak potentials ( $\Delta E_p$ ) increased with scan rate and the average of the peak potentials, 1/2(*E*<sub>p,c</sub> + *E*<sub>p,a</sub>) was more or less constant for different scan rates, indicating that the reduction process is quasi-reversible [34, 35].

The heterogeneous electron transfer rate constant, *k*<sub>s</sub> could be calculated using Eq. (4), which was proposed by Klingler and Kochi [36] based on peak separation.

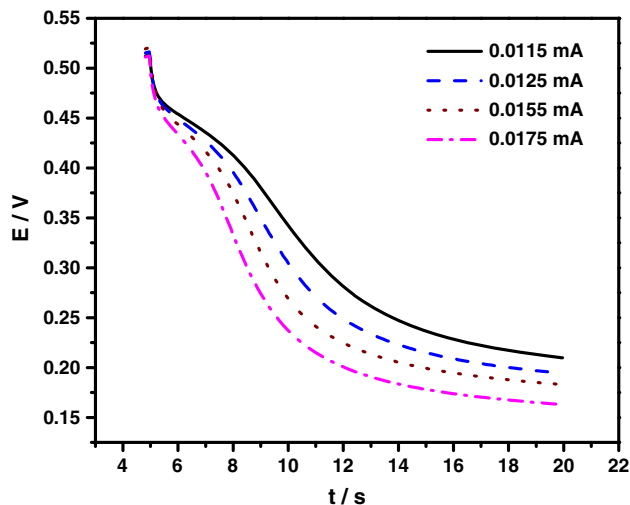


**Fig. 7** Chronopotentiograms recorded for [RuNO]<sup>3+</sup> ions in 1 M HNO<sub>3</sub> at different applied currents; [Ru]: 40 mM; WE: Pt; CE: Pt; RE: Ag/AgCl

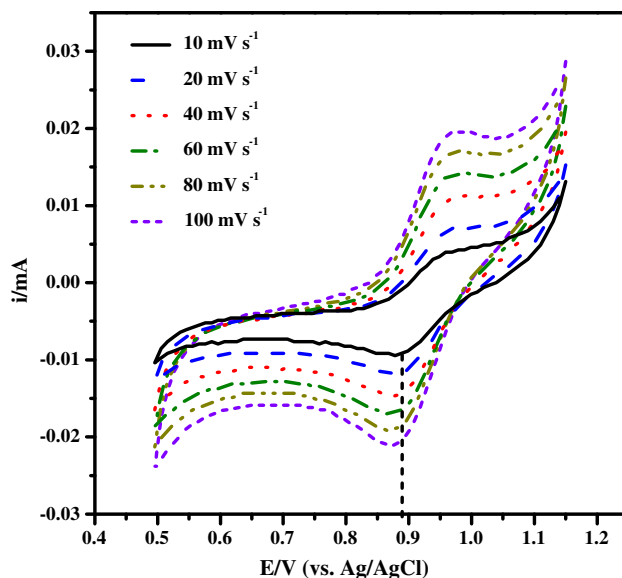


**Fig. 8** Cyclic voltammograms of 40 mM [RuNO]<sup>3+</sup> solution in 1 M nitric acid recorded using GC electrode with different scan rates at 298 K; CE: Pt; RE: Ag/AgCl

**Table 2** Peak parameters obtained for 40 mM [RuNO]<sup>3+</sup> solution in 1 M HNO<sub>3</sub> from the CVs recorded with GC working electrode

Scan rate/mV s <sup>-1</sup>	<i>E</i> <sub>p,c</sub> /V	<i>i</i> <sub>p,c</sub> /A	<i>E</i> <sub>p,a</sub> /V	( <i>E</i> <sub>p,a</sub> – <i>E</i> <sub>p,c</sub> )/V	[1/2( <i>E</i> <sub>p,c</sub> + <i>E</i> <sub>p,a</sub> )]/V
10	0.892	–5.9 × 10 <sup>-6</sup>	0.959	0.067	0.93
20	0.885	–6.7 × 10 <sup>-6</sup>	0.969	0.084	0.93
40	0.879	–1.1 × 10 <sup>-5</sup>	0.975	0.096	0.93
60	0.869	–1.2 × 10 <sup>-5</sup>	0.981	0.112	0.93
80	0.864	–1.4 × 10 <sup>-5</sup>	0.984	0.120	0.92
100	0.860	–1.5 × 10 <sup>-5</sup>	0.989	0.129	0.92

$$k_s = 2.18 \left[ D_0(\alpha n_\alpha) \frac{vF}{RT} \right]^{1/2} \exp \left[ \frac{\alpha^2 nF}{RT} (E_p^c - E_p^a) \right]. \quad (4)$$

According to Eq. (4), if  $[k_s/(v)^{1/2}] > 0.11$ , the process is reversible. If  $0.11 > [k_s/(v)^{1/2}] > 3.7 \times 10^{-6}$ , then it is quasi-reversible. If  $3.7 \times 10^{-6} > [k_s/(v)^{1/2}]$ , the process is irreversible. The value of  $k_s$  calculated for the scan rate of 10 mV s<sup>-1</sup>, using  $D_0 = 2.95 \times 10^{-8}$  cm<sup>2</sup> s<sup>-1</sup> was  $2.06 \times 10^{-5}$  cm s<sup>-1</sup> and the value of  $[k_s/(v)^{1/2}]$  obtained for the same scan rate was  $2.06 \times 10^{-4}$  cm s<sup>(-1/2)</sup> V<sup>(-1/2)</sup>. These values imply that the reduction of [RuNO]<sup>3+</sup> ion is quasi-reversible.

### 3.3 Chronopotentiometric study on the reduction of ruthenium nitrosyl ions

The chronopotentiograms of 40 mM ruthenium in [RuNO]<sup>3+</sup> solution in 1 M HNO<sub>3</sub>, recorded at Pt electrode for various applied constant current are shown in Fig. 7. The transient time ( $\tau$ ) in the chronopotentiogram is a measure of time elapsed between the attainment of constant potential and the time at which the concentration of electro-active species (resulting from diffusion) reaches zero at the electrode. A relation between the applied current and transient time is given by Sand's equation [33], which enables the determination of diffusion coefficient.

$$i\tau^{1/2} = \frac{nFA(D_0\pi)^{1/2}}{2} C_0. \quad (5)$$

The  $D_0$  value of  $1.1 \times 10^{-8}$  cm<sup>2</sup> s<sup>-1</sup> derived using Eq. (5) at room temperature is in reasonably good agreement with the value of diffusion coefficient calculated from cyclic voltammetric results.

### 3.4 Reduction of [RuNO]<sup>3+</sup> moiety using glassy carbon (GC) working electrode

The cyclic voltammograms recorded for a solution of [RuNO]<sup>3+</sup> containing 40 mM Ru in 1 M HNO<sub>3</sub> at different scan rates, using GC as the working electrode at 298 K are shown in Fig. 8. The redox behaviour exhibited by [RuNO]<sup>3+</sup> in 1 M HNO<sub>3</sub> at GC electrode was similar to that at Pt electrode. However, the reduction wave for

[RuNO]<sup>3+</sup> complex was observed to occur at lower cathodic potentials (0.9 V vs. Ag/AgCl) with GC working electrode than that of 0.45 V versus Ag/AgCl with Pt WE, for the scan rate of 10 mV s<sup>-1</sup>. The peak parameters measured from the cyclic voltammograms using GC as the working electrode are listed in Table 2.

The peak potential shift and broadening of peak shape with scan rate in CV, observed using GC electrode were similar to the behaviour of the CVs at Pt electrode. The difference between the cathodic and anodic peak potentials ( $\Delta E_p$ ), increased with scan rate and the average of the peak potentials,  $\frac{1}{2}(E_{p,c} + E_{p,a})$  was nearly constant for different scan rates, suggesting that the process could be quasi-reversible. The value of diffusion coefficient calculated on the basis of Eq. (3) was  $1.65 \times 10^{-8}$  cm<sup>2</sup> s<sup>-1</sup> for the reduction of [RuNO]<sup>3+</sup> moiety at GC electrode, which is in good agreement with the value of  $2.95 \times 10^{-8}$  cm<sup>2</sup> s<sup>-1</sup> obtained at Pt electrode.

The potential versus time transients for the reduction of [RuNO]<sup>3+</sup> ions at GC electrode is shown in Fig. 9. Using Eq. (5),  $D_0$  of [RuNO]<sup>3+</sup> at GC electrode was determined to be  $1.57 \times 10^{-8}$  cm<sup>2</sup> s<sup>-1</sup>, which is in excellent agreement with the value of  $1.1 \times 10^{-8}$  cm<sup>2</sup> s<sup>-1</sup>, obtained at Pt electrode using Eq. (5). The heterogeneous electron transfer rate constant,  $k_s$  ( $6.73 \times 10^{-5}$  cm s<sup>-1</sup>), obtained at GC

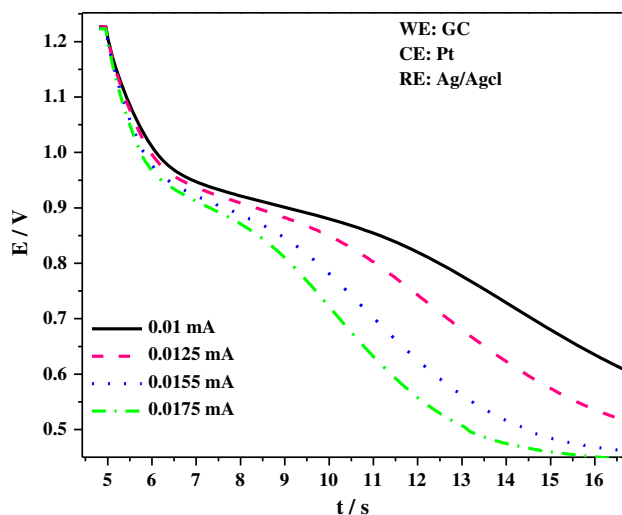


**Fig. 9** Chronopotentiograms of 40 mM [RuNO]<sup>3+</sup> solution in 1 M HNO<sub>3</sub> recorded at GC electrode with different applied current

**Table 3** Comparison of kinetic parameters derived for the reduction of  $[\text{RuNO}]^{3+}$  species in 1 M  $\text{HNO}_3$  at Pt and GC working electrodes

Kinetic parameters	40 mM $[\text{RuNO}]^{3+}$ solution in 1 M $\text{HNO}_3$	
	Platinum	Glassy carbon
$D_0$ ( $\text{cm}^2 \text{s}^{-1}$ )/CV expt.	$2.95 \times 10^{-8}$	$1.65 \times 10^{-8}$
$D_0$ ( $\text{cm}^2 \text{s}^{-1}$ )/CP expt.	$1.1 \times 10^{-8}$	$1.57 \times 10^{-8}$
$k_s$ ( $\text{cm s}^{-1}$ )/Eq. (4)	$2.06 \times 10^{-5}$	$6.73 \times 10^{-5}$

electrode also indicates the reduction of  $[\text{RuNO}]^{3+}$  in 1 M nitric acid to be quasi-reversible.

The value of heterogeneous electron transfer rate constant ( $k_s$ ), estimated using Klingler and Kochi equation [36] and the diffusion coefficient values determined from the results of CV and CP for the reduction of  $[\text{RuNO}]^{3+}$  species in 1 M  $\text{HNO}_3$  at the working electrodes Pt and GC are compared in Table 3. The data in Table 3 reveal the redox behaviour of  $[\text{RuNO}]^{3+}$  solution in 1 M  $\text{HNO}_3$  to be the same with both electrodes.

#### 4 Conclusions

The reduction behaviour of  $[\text{RuNO}]^{3+}$  species in nitric acid medium was investigated by CV and CP using Pt as well as GC working electrodes. Quasi-reversible, one electron reduction of  $[\text{RuNO}]^{3+}$  ion was observed at both electrodes. The diffusion coefficient ( $D_0$ ) of  $[\text{RuNO}]^{3+}$  species, determined by CV and CP techniques was in the order of  $10^{-8} \text{ cm}^2 \text{ s}^{-1}$  and the heterogeneous electron transfer rate constant ( $k_s$ ) for the reduction of  $[\text{RuNO}]^{3+}$  was estimated to be in the order of  $10^{-5} \text{ cm s}^{-1}$  using Klingler and Kochi equation. The very low diffusion coefficient value revealed the complexing nature of Ru(II). As Ru(II) exists as different complexes instead of bare Ru(II) ions in nitric acid medium, the separation percentage of Ru from ruthenium nitrosyl nitrate solution by electro-deposition technique will be very low. Hence, it is advantageous to separate and recover Ru as  $\text{RuO}_4$  from liquid waste, by electro-oxidation method.

**Acknowledgments** Ms. Pravati Swain acknowledges the financial support provided by Department of Atomic Energy in the form of Research Fellowship.

#### References

- Fletcher JM, Jenkins IL, Lever FM, Martin FS, Powell AR, Todd R (1955) Nitrate and nitro complexes of nitrosylruthenium. *J Inorg Nucl Chem* 1:378–401
- Brown PGM (1960) Nitro complexes of nitrosylruthenium. *J Inorg Nucl Chem* 13:73–83
- Wallace RM (1961) The composition of some nitrate nitrosylruthenium complexes. *J Inorg Nucl Chem* 20:283–289
- Balcerzak M (2002) Analytical methods for the determination of ruthenium: the state of the art. *Crit Rev Anal Chem* 32:181–226
- Scargill D, Lyon CE, Large NR, Fletcher JM (1965) Nitrate complexes of nitrosyl ruthenium III. *J Inorg Nucl Chem* 27:161–171
- Siczek AA, Steindler M (1978) The chemistry of ruthenium and zirconium in the PUREX solvent extraction process. *At Energy Rev* 16:575–618
- Boswell GJJ, Soentono S (1981) Ruthenium nitrosyl complexes in nitric acid solutions. *J Inorg Nucl Chem* 43:1625–1632
- Swain Pravati, Mallika C, Srinivasan R, Kamachi Mudali U, Natarajan R (2013) Separation and recovery of ruthenium—a review. *J Radioanal Nucl Chem* 298:781–796
- Bockris JO'M, Kim J (1997) Electrochemical treatment of low-level nuclear wastes. *J Appl Electrochem* 27:623–634
- Molenda E, Mielcarski M (1998) Electrodeposition of  $^{106}\text{Ru}$  and  $^{241}\text{Am}$  and derived information on preparing sealed radiation sources. *J Radioanal Nucl Chem* 238:159–162
- Ozawa M, Shinoda Y, Sano Y (2002) The separation of fission-product rare elements toward bridging the nuclear and safety energy systems. *Prog Nucl Energy* 40:527–538
- Ozawa M, Suzuki T, Koyama S, Fujii Y (2005) Separation of rare metal fission products in radioactive wastes in new directions of their utilization. *Prog Nucl Energy* 47:462–471
- Jayakumar M, Venkatesan KA, Srinivasan TG, Vasudeva Rao PR (2010) Feasibility studies on the electrochemical recovery of fission platinoids from high-level liquid waste. *J Radioanal Nucl Chem* 284:79–85
- Jayakumar M, Venkatesan KA, Sudha R, Srinivasan TG, Vasudeva Rao PR (2011) Electrodeposition of ruthenium, rhodium and palladium from nitric acid and ionic liquid media: recovery and surface morphology of the deposits. *Mater Chem Phys* 128:141–150
- Turner AD (1989) Liquid treatment process. US Patent 4879006
- Motojima K (1990) Removal of Ru from PUREX process. *J Nucl Sci Technol* 27:262–266
- Motojima K (1990) Process for removing radioactive ruthenium from aqueous solution. US Patent 4938895
- Yoneya M, Kawamura K, Torata SI, Takahashi T (1995) Method of separating and recovering ruthenium from high-level radioactive liquid waste. US Patent 5437847
- Mousset F, Bedioui F, Eysseric C (2004) Electroassisted elimination of Ru from dissolved  $\text{RuO}_2 \cdot x\text{H}_2\text{O}$  in nitric acid solution using Ag(II) redox mediator. *Electrochem Commun* 6:351–356
- Pravati Swain, Mallika C, Sankaran K, Pandey NK, Srinivasan R, Kamachi Mudali U, Natarajan R (2014) Feasibility studies on the separation of ruthenium from high level liquid waste by constant potential electro-oxidation. *Prog Nucl Energy* 75:198–206
- Toledo JC Jr, Lopes LGF, Alves AA, da Silva LP, Franco DW (2002) Release of NO by a nitrosyl complex upon activation by the mitochondrial reducing powder. *J Inorg Biochem* 89:267–271
- Borges SSS, Davanzo CU, Castellano EE, Z-Schepeter J, Silva SC, Franco DW (1998) Ruthenium nitrosyl complexes with *N*-heterocyclic ligands. *Inorg Chem* 37:2670–2677
- Lang DR, Davis JA, Lopes LGF, Ferro AA, Vasconcellos LCG, Franco DW, Tfouni E, Wieraszko A, Clarke MJ (2000) A controlled NO-releasing compound. *Inorg Chem* 39:2294–2300
- Gomes MG, Davanzo CU, Silva SC, Lopes LGF, Santos PS, Franco DW (1998) *Cis*- and *trans*- nitrosyltetraammineruthenium (II). Spectra and electrochemical properties and reactivity. *J Chem Soc Dalton Trans* 4:601–608
- Lopes LGF, Gomes MG, Borges SSS, Franco DW (1998) Correction to lever parameter and electronic properties of nitrosyl ruthenium (II) complexes. *Aust J Chem* 51:865–866
- McGarvey BR, Ferro AA, Tfouni E, Brito Bezerra CW, Bagatin I, Franco DW (2000) Detection of the EPR spectra of NO in Ruthenium (II) complexes. *Inorg Chem* 39:3577–3581

27. Leon M (1979) Ruthenium (IV) in nitric acid media. *J Inorg Nucl Chem* 41:67–71
28. Bailar JO (ed) (1973) *Comprehensive inorganic chemistry*. Pergamon Press, Oxford
29. Cotton SA, Hart FA (1975) *The heavy transition elements*. Wiley, New York
30. Tfouni E, Krieger M, McGarvey BR, Franco DW (2003) Structure, chemical and photochemical reactivity and biological activity of some ruthenium amine nitrosyl complexes. *Coord Chem Rev* 236:57–69
31. Doro FG, Filho UPR, Tfouni E (2007) A regenerable ruthenium tetraammine nitrosyl complex immobilized on a modified silica gel surface: preparation and studies of nitric oxide release and nitrite to NO conversion. *J Colloid Interface Sci* 307:405–417
32. Duchovnay A (2011) Comparative electrochemistry, electronic absorption spectroscopy and spectroelectrochemistry of the monometallic ruthenium polypyridyl complexes. Dissertation (MS), Virginia Polytechnic Institute and State University, Blacksburg
33. Bard AJ, Faulkner LR (2001) *Electrochemical methods—fundamentals and applications*, 2nd edn. Wiley, New York
34. Jagadeeswara Rao Ch, Venkatesan KA, Nagarajan K, Srinivasan TG, Vasudeva Rao PR (2009) Electrochemical behavior of europium (III) in *N*-butyl-*N*-methylpyrrolidinium bis(trifluoromethylsulfonyl)imide. *Electrochim Acta* 54:4718–4725
35. Jagadeeswara Rao Ch, Venkatesan KA, Nagarajan K, Srinivasan TG, Vasudeva Rao PR (2010) Electrochemical and thermodynamic properties of europium(III), samarium(III) and cerium(III) in 1-butyl-3-methylimidazolium chloride ionic liquid. *J Nucl Mater* 399:81–86
36. Klingler RJ, Kochi JK (1981) Electron transfer kinetics from cyclic voltammetry. quantitative description of electrochemical reversibility. *J Phys Chem* 85:1731–1741